https://doi.org/10.18406/2316-1817v15n120231723 e-ISSN 2316-1817

Modeling of the land surface temperature as a function of the soil-adjusted vegetation index

Luis Carlos da Silva Soares[1], Philipe Guilherme Corcino Souza[2], Sarah Dieckman Assunção Rodrigues[3], Rafaela Carla Santos Perpétuo[4], Isadora Azevedo Perpétuo[5]

[1] Universidade Federal de Lavras, Departamento de Ciências Naturais, Doutorando. luisccbvgp@gmail.com
[2] Universidade Federal dos Vales do Jequitinhonha e Mucuri, Departamento de Produção Vegetal, Doutorando. philipe.corcino@gmail.com
[3] Universidade Federal de Lavras, Departamento de Ciências do Solo, Mestrando. sarahdieckman.a.r@gmail.com
[4] Instituto Federal de Minas Gerais, Departamento de Ciências Florestais, Engenheira Florestal. rafaela.perpetuo@outlook.com
[5] Universidade Federal de Lavras, Departamento de Ciências Florestais, Mestrando. isadoraperpetuo@homail.com

Recebido em: 12/05/2022
Aceito em: 24/10/2022

Abstract

Land surface temperature is a physical-environmental variable that is the target of studies in climatology and heat island phenomena resulting from the urbanization model of the 21st century. It is known that each object has a different thermal capacity, which results in higher or lower temperatures. The modeling of temperature as a function of objects on the land surface can allow understanding between these variables. It can corroborate temperature forecasts with the alteration of objects in an area. The objects on the Earth's surface can be computed with geoprocessing techniques that aim to detail Land Use and Occupation. This paper evaluates the Linear, Exponential, and Sinusoidal models to determine which of these models is more expressive for the study of the land surface temperature as a function of land surface objects. For this purpose, images from the Landsat 8 satellite were used to calculate the Earth's surface temperature and determine the scene's objects. To determine the scene's objects, the Soil Adjusted Vegetation Index (SAVI) was used, which is one of the techniques for obtaining Land Use and Occupation. For model analysis, Akaike's Information Criterion (AIC), Bayesian Information Criterion (BIC), and Sum of Square of Residuals (SSR). According to the AIC, BIC, and SSR criteria, the sinusoidal model presented better performance when compared to the other models. However, there are large variations in SSR between classes, especially for the pasture class, which makes the models not highly explanatory.

Keywords: Geoprocessing. Landsat. Land Use and Occupation.

Introduction

In Climatology, there is an effort to understand the relationship between Land Use and Land Occupation with land surface temperature (LST), driven mainly by the growing anthropization of the landscape and global warming. Understanding the relationship between these variables can have direct implications on the urbanization model of the 21st century, generating projections of scenarios for heat islands and ecosystem studies (XU & TAN, 2007; WENG *et al.,* 2014). However, the great challenge has been to find explanatory models that express the dependence of surface temperature on the constituents of the scene, especially models that use water bodies (BEZERRA *et al.,* 2018).

The LST is characterized as a heat flow of a given body as a function of the difference in energy absorbed by the radiated energy, allowing us to understand better the interaction of the Earth's surface and the atmosphere (STEINKE *et al*., 2010). Such metric subsidizes studies of thermal patterns of landscapes, the survey of evapotranspiration of crops and forests, heat island diagramming, and assessment of soil moisture, besides being an essential tool for the evaluation of environmental, ecological, and climatic processes in a local, regional and global sphere (WENG et al., 2014; FERREIRA *et al.,* 2020; PIRES; VALLERIUS, 2020).

The estimate of LST is based on Planck's law (1901) in which everybody that is not at absolute zero emits different values of electromagnetic radiation. In turn, this radiation can be captured by sensors and converted into temperature by remote sensing techniques (BALDU, 2006).

Therefore, it is possible to infer a relation of the LST as a function of each body.

To understand LST related to each landscape constituent, it is necessary to survey them at the study site. Generally, these objects can be distributed in areas of exposed soil, vegetated areas, and areas with water bodies. Studies that seek this premise use land use and occupation survey techniques using vegetation indices (CRUZ, 2019). Among the various existing vegetation indices, the Soil Adjusted Vegetation Index (SAVI) deserves prominence for minimizing the interference of soil values making the classification more accurate (SILVA & GAVINCIO, 2012).

The modeling of the LST as a function of land use and occupation can contribute to predicting the temperature for an area if there is a modification of the landscape. Predict the behavior of temperature can be a crucial tool in decision-making and monitoring of ecological succession processes and soil microbiota (MOREIRA & SIQUEIRA, 2006), in addition, to being able to subsidize microclimate studies since LST promotes the loss of moisture at the surface by evaporation (CARNEIRO, 2014).

Traditionally, studies relating land use and occupation with LST employ mostly linear models, as seen by Marques et al. (2005), Araújo et al. (2017), Bezerra et al. (2018), and Becker et al. (2020). However, the quality of this model shows variation among some literature, obtaining good performance in some studies and others not. Moreover, employing the linear model in the modeling of LST and land use and occupation considering the presence of water bodies has been a challenge since they do not present satisfactory results due to the particularity of their thermal and optic properties (SOARES *et al*.,2020).

Although there is variation in the relationship between land use and occupation with LST when using the linear model, such a relationship may be better expressed as a function of non-linear models. This paper evaluated the LST as a function of land use and occupation through the traditional linear model and non-linear exponential and sinusoidal models.

Material and methods

Study area

The study area was the municipality of Governador Valadares, located in Doce River Valley, the eastern region of the state of Minas Gerais in the coordinates Latitude 18 ° 51'2 "S; Longitude: 41°56'53" E (Figure 1). It is located in the Atlantic Forest biome (Figure 2), with an altitude of 180 meters above sea level and a tropical climate classified as AW-type sub-hot and sub-dry tropical (KÖPPEN, 1948). Its temperature is high, it reaches a historical mean of 26.9ºC in summer and 21.5ºC in winter. Mean annual rainfall and relative humidity are 1,113.80 mm and 75%, respectively (PMSB, 2015).

The choice of the municipality was due to its spatial heterogeneity. It has a total area of 2,342,325 km2, 57.59 km^2 of urban area (IBGE, 2018). The municipality has areas of Atlantic Forest, areas of exposed and degraded soil (FAVERO, 2001), pasture area, and the River Doce (Rio Doce) presence. It presents Ombrophilous Dense forests in higher areas and Seasonal Semideciduous and Deciduous composition in lower and dissected areas (PMSB, 2015). Its location on the bank of the Doce River favored the city's demographic expansion and the intense use of natural resources, especially mineral and forest exploration, which created long-term environmental issues (ESPÍNDOLA, 2015). The heterogeneity of the landscape, which is composed of different Land Use and Occupation Classes, was the main characteristic of the analysis for LST estimation.

Figure 1- Location of the study area.

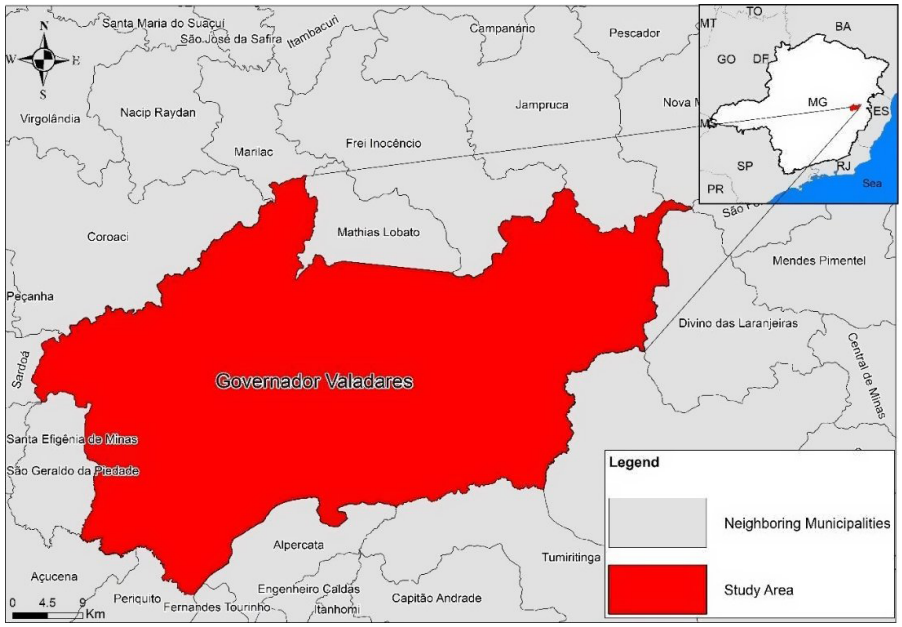

Source: Prepared by the authors (2023).

Figure 2- Biome in the study area.

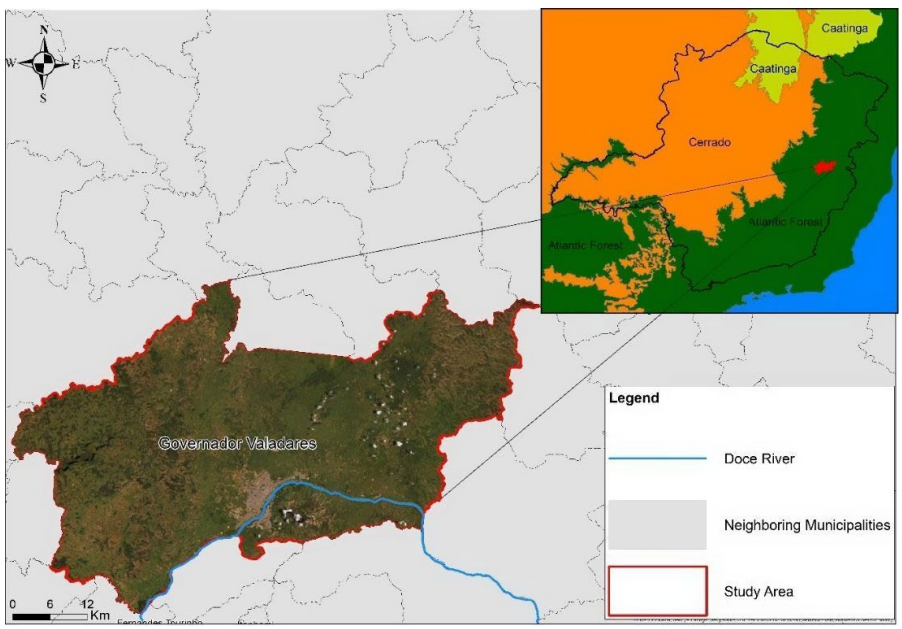

Source: Prepared by the authors (2023).

Work steps

The study was developed from the acquisition of a Landsat 8 satellite image of orbits and points 216/73 and 217/73, respectively on the date of 12/04/2020. The images were acquired from the United States Geological Service Site (USGS).

Digital Image Processing (DIP)

Initially, the Bands' radiometric correction was performed to reduce the interference of the atmosphere and correct errors inherent to the satellite calibration. The conversion of the digital values (DV) of the images into radiance values

was performed with the help of the Software ENVI 5.1 (2011). Later, Band 8 (Panchromatic) was merged with the other OLI Sensor bands to improve the Images' resolution. Then, bands 2,3,4,5, 10, and 11 of each scene were merged, each with its corresponding one. Each newly generated band was cut using the shapefile of the municipality (IBGE, 2020). In the end, the reprojection of the Bands from the northern hemisphere to the southern hemisphere was carried out and the processing for the estimation of LST was followed.

Land Surface Temperature Calculation (LST)

To calculate LST Band 10 corresponding to the thermal infrared range (10.6 - 11.19 μm) captured by the TIRS sensor was used. This band is used because it contains infrared values emitted as a function of their temperature by objects, in addition to suffering little interference in the atmosphere (GUSSO *et al.*, 2007; BORGES & OLIVEIRA, 2010). To determine the Spectral Radiance Equation (1) and LST Equation (2) the methodology of Coelho & Correa (2013) was used. The values of each element and constant were extracted from the metadata file provided with the raster.

$$L\lambda = ML \cdot QCAL + AL \qquad \text{Equation (1)}$$

Where: Lλ = Aperture Sensor Spectral Radiance in Watts/ (m^2 sr μm); ML = Band 10 resize multiplicative factor; QCAL = Band-specific additive scaling factor; AL = Digital band level values, it is the input of the band itself.

$$T = K2 \div \ln\left(k1 \div L\lambda + 1\right) \qquad \text{Equation (2)}$$

Where: T = Effective temperature on the satellite in Kelvin (K); K2 = Band 10 resize multiplicative factor; K1 = Band 10 specific additive resizing factor; Lλ = Spectral radiance in Watts/ (m^2 sr μm).

The temperature obtained by $T = K2 \div ln\left(k1 \div L\lambda + 1\right)$ Equation (2) was converted to degrees Celsius (°C) by subtracting the value found by the temperature of the freezing point of water at 1 atm (273.15K).

Soil Adjusted Vegetation Index (SAVI)

The calculation of SAVI, used by Huete (1988), is described by Equation 3. The objective is to classify the objects present in the scene in an output interval between -1 to $+1$, using Landsat 8 OLI red (Band 4) and near-infrared (Band 5) bands. The model is like the one used to calculate the Normalized Difference Vegetation Index (NDVI), differentiating itself by adding an Ls correction to minimize the effects of soil values and improve the accuracy for areas without uniform vegetation cover (HUETE & LIU; 1994). The correction value was based on the studies by Huete & Liu (1994) using Ls equal to 0.5 due to the heterogeneity of objects in the scene composition.

$$SAVI = \left(BAND5 - BAND4\right) \cdot \left(1 + Ls\right) \div \left(BAND5 + BAND4 + Ls\right) \qquad \text{Equation (3)}$$

Where: BAND 4 = Spectral Band Red; BAND 5 = Near-infrared spectral band; Ls = Constant called the adjustment factor of the SAVI index.

Classification of Ground Objects

For a better classification of Object Classes present in the scene, an RGB combination of Bands 5 (Red), Band 4 (Green), and Band 3 (Blue) of the Landsat 8 satellite was performed. In the sampling process described above, it was verified in which class the measured SAVI and LST belonged to validate the data. The criteria used were described in Table 1.

Statistical Models

For all models tested in this paper, LST was modeled as a function of SAVI. For modeling purposes, the statistical program R Development Core Team (2020) and CurveExpert (HYAMS, 2020) were used. The CurveExpert software was used to estimate the values of the initial parameters of the models shown in Table 2. These values were then used in the R software for statistical analysis of the models and their

Table 1- Soil classes as a function of SAVI sampled.

SAVI interval	Land use types
$x \leq 0$	Waterbody
$0 < x \leq 0.25$	Region without Vegetation
$0.25 < x \leq 0.45$	Pasture region and sparse vegetation
$x > 0.45$	Native forest/ Dense Vegetation

Where x = SAVI value.

Source: Prepared by the authors (2023).

Table 2- Statistical Models used in LST modeling as a function of SAVI.

MODEL	Model Equation
Linear (Model 1)	$y = b0 + b1 \cdot x$
Exponential (Model 2)	$y = b0 + e^{b1*x}$
Sinusoid (Model 3)	$y = b0 + b1 \cdot \cos\left(b2 \cdot x \cdot + b3\right)$

Where: b0, b1, b2, and b3 are model parameters. e= Euller number. x= SAVI and Y= LST C

Source: Prepared by the authors (2023).

validation K-fold following the procedures available on https://github.com/Luigicarlo01/LST-SAVI/blob/main/Validation.

Two distinct modeling groups were evaluated. The first considers SAVI with all Ground Classes. The second disregards the SAVI water bodies in the modeling. The justification for removing water bodies comes from the anomalous behavior of water in emissivity, reflectance, radiation absorption, and radiation scattering (FERREIRA & FILHO, 2009), which causes lower SAVI values to present a median temperature as a function of its specific heat.

Model evaluation

The evaluation of the models was based on the recommendations of Zeviani et al. (2013). The Akaike Information Criterion (AIC), Bayesian Information Criterion (BIC), and Sum of squares of the residuals (SSR) were determined.

Results and discussion

The parameters of the evaluated models were significant in the "t" test, presenting a $p < 0.05$ as shown in Table 3. It is noted that parameter b1 for the linear and Exponential models has a negative value, both for models that use hydrous bodies in modeling and those that do not, indicating that the temperature decreases as the SAVI increases.

Within the models using data from water bodies, it was found that the sinusoidal model presented the best parameters of AIC, BIC, and SSR, having the lowest values when compared to the other models (Table 4). The SSR of the sinusoidal model was almost three times smaller than the Linear and Exponential models, which may indicate that the latter does not explain well the relationship between SAVI and Earth's Surface Temperature.

Models whose modeling did not use waterbody data also showed better values for the sinusoidal model, with lower values in the AIC, BIC, and SSR. However, unlike the modeling that inserts data from historical bodies, these parameters are close values between models. In addition, comparing the SSR values of models that use water bodies with those that do not use water bodies, a decrease is observed when the

Table 3: Information on the parameters of the Linear, Sinusoidal, and Exponential models considering modeling with and without water bodies.

MODEL WITH WATER BODIES	Value	Error	t	p
		b0		
Linear	26,3757	0,1613	163,484	<0,0001
Exponential	26,3459	0,1612	163,454	<0,0001
Sinusoid	26,1802	0,0668	392,14	<0,0001
		b1		
Linear	-2,3104	0,4483	5,154	<0,0001
Exponential	-0,0852	0,0173	4,926	<0,0001
Sinusoid	-2,2721	0,0837	27,16	<0,0001
		b2		
Sinusoid	8,7462	0,2254	38,81	<0,0001
		b3		
Sinusoid	-1,9506	0,0845	23,09	<0,0001
MODEL WITHOUT WATER BODIES	**Value**	**Error**	**t**	**p**
		b0		
Linear	29,2443	0,1676	174,52	<0.0001
Exponential	29,4146	0,1772	166,03	<0.0001
Sinusoid	26,3643	0,1195	220,553	<0.0001
		b1		
Linear	-9,4391	0,4371	21,59	<0.0001
Exponential	-0,3652	0,0166	22,02	<0.0001
Sinusoid	2,2306	0,0987	22,604	<0.0001
		b2		
Sinusoid	7,2025	0,6068	11,87	<0.0001
		b3		
Sinusoid	-0,5356	0,2529	2,118	<0.0001

Where: b0, b1, b2 e b3 are parameters of models. t = t value and p = p-value.

Source: Prepared by the authors (2023).

Table 4: Model Comparison Parameters.

Models with water bodies			
PARAMETER	LINEAR	EXPONENTIAL	SINUSOID
AIC	1490,967	1492,207	1119,593
BIC	1502,541	1503,781	1138,882
SSR	1353,327	1415,65	488,031
Models without water bodies			
AIC	1026,06	1031,263	988,6878
BIC	1037,171	1042,374	1007,207
SSR	534,3536	526,4227	458,611

Where: AIC, BIC e SSR are the Akaike information criterion, Bayesian information criterion, and the sum of squares of the residuals, respectively.

Source: Prepared by the authors (2023).

scene water bodies values are disregarded. This decrease is more explicit in linear and exponential models, with an almost 3-fold reduction in total residuals.

The graphical analysis of the data plotted for the observed values and values estimated by the modeling corroborate the information mentioned above. Visually, it is observed that for the modeling with water bodies Figure 3-A, the sinusoidal model was able to better contemplate the values of the observations compared to the Linear and Exponential Models. The latter showed similar behavior to each other with an overlapping of the lines. This also corroborates the data in the previous table, where it is shown that the AIC, BIC, and SSR parameters are similar.

The graphical analysis of the plotted data that does not consider the values of the waterbodies in the modeling, as can be seen in Figure 3-B presents an overlapping behavior of the lines for the exponential and linear models. However, unlike Figure 3-A, these models considered the SAVI values in the range that corresponds to the exposed soil (0.0 <SAVI <0.25).

The higher temperatures in this class can be explained by the specific heat inherent to the type of soil in the studied area. The soils of Governador Valadares are predominantly composed of clayey oxisol (ALBUQUERQUE et al., 2008), having a specific heat of magnitude 0.2127 cal. g C^{-1} (OKE, 1995). The closer to zero the value, the greater the energy needed to vary the temperature of a body causing it to heat up faster, obtaining the highest temperatures.

As the vegetation gradient moves closer to 1, the vegetated area becomes denser. In this process, it is noted that the temperature tends to decrease as the vegetation becomes denser. The explanation for this result may come from the presence of a water gradient in the leaves of the plants. Water has a specific heat of approximately 1 cal / g. °C means that the energy given to the

Figure 3: Adjusted temperature models as a function of SAVI considering water bodies (A) and without water bodies (B).

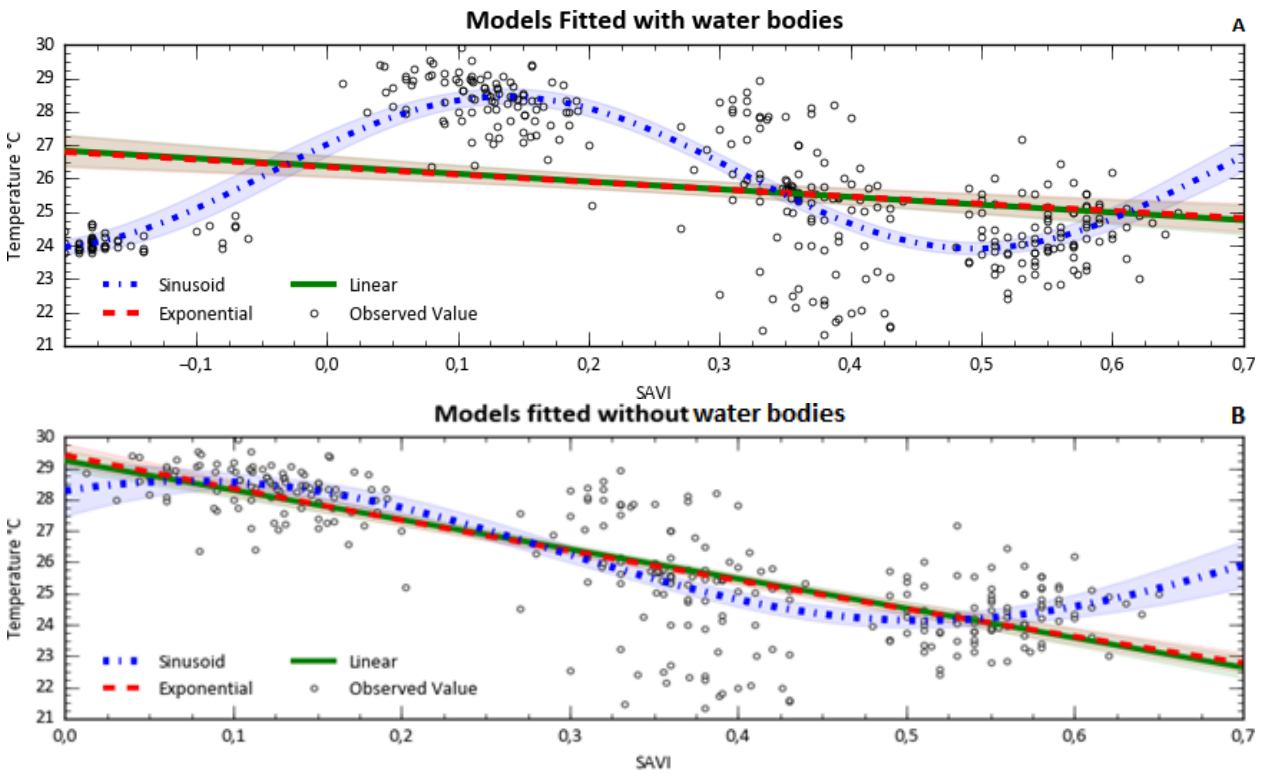

Source: Prepared by the authors (2023).

system must be greater for its temperature to vary. Therefore, the water is more difficult to be heated, causing the system temperature to vary less, and consequently, to have a lower temperature (PILLAR, 1995; BATALHA, 2011; BARBOSA *et al*., 2019). This justification for denser bodies can be confirmed by observing the similarity of the temperature of denser vegetation (SAVI> 0.45) with places that contain only water bodies SAVI <0.0 (Figure 3-A).

The range of SAVI corresponding to pasture (2.50 <SAVI <4.50) showed a wide dispersion of observed values (Figure -A-B). Pereira et al. (2012) found in their work temperature variations for pasture areas 18.8 ° C - 31.1 ° C. According to the authors, this variation may result from pasture degradation, increasing an exposed soil area. As the soil has a lower specific heat than plants, the temperature of these points tends to be higher. This variation may be responsible for the high SSR values for the class, as shown in Table 5.

The SSR of the class, shown in Table 5, demonstrates variation within each model. High-class values indicate an inadequate fit of the class to the model. High standard deviations indicate significant variations between classes for a given model. The Models assessed showing high standard deviation for an SSR demonstrate the model does not explain a temperature variable within all classes.

The SSR analysis for modeling without water bodies shows lower values of total SSR and standard deviation when compared to modeling with water bodies. Although these models may be better, they also have a somewhat high standard deviation between classes, which may be due to the pasture class. Thus, models may not fit well in the values of this class, implying greater prediction errors.

One way to get around this problem would be to adopt modeling by individual classes. In this way, each class would have its own model, and these would not interfere with the other models' values. Thus, the accuracy may be greater.

Limitations of the study

This work evaluated as a predictor variable for surface temperature the SAVI value of a single scene. The tested models deal only with

Table 5: SSR of classes by evaluated model

Models with Water bodies			
CLASS	**LINEAR**	**EXPONENTIAL**	**SINUSOID**
Exposed Soil	593,5362	643,9028	133,9308
Pasture	298,2384	305,4197	253,1735
Dense Vegetation	124,7141	132,4717	86,0275
Water	336,8382	333,8558	14,8713
standard deviation	193,5386	212,8256	100,1988
Total	1353,327	1415,65	488,0031
Models without Water bodies			
Exposed soil	135,5888	156,3396	113,5632
Pasture	287,8216	269,3596	265,5283
Dense Vegetation	110,9432	100,7235	79,5195
standard deviation	78,22205	70,16236	80,86452
Total	534,3536	526,4227	458,611

Source: Prepared by the authors (2023).

only one variable, and it is not possible to use multiple characteristics directly within these models. It is possible to study two characteristics simultaneously for temperature prediction using covariance between characteristics as the predictor.

More robust image processing techniques and data analysis can be more useful for handling a large amount of data and plotting a model using multiple characteristics. In this scenario, the use of Neural Networks and machine learning may present themselves as alternatives for improving the results.

The models in this study present only concern the study area not being validated for other regions. The equations found were not tested in other regions. Therefore, its use is not recommended to estimate the temperature of other sites. Further studies validating the equations for other locations, within the biome itself and in others, it is important to verify the possibility of using the model only on a local scale or in a large region.

Final considerations

There was a significant variation of residues for the exposed soil and water bodies Class in the linear and exponential models. In contrast, the exposed soil presented the highest value for all models in the modeling without the water bodies.

It was verified that the models tested in the modeling of the Land Surface Temperature with the Use and Occupation of the Land with and without water bodies need more study for a better adaptation. Although the Sinusoid model was better in the AIC, BIC, and SSR parameters, the residual analysis showed a non-homogeneous distribution and high values. These residual values imply an underestimation and overestimation of the Temperature values, compromising the model's efficiency.

References

ALBUQUERQUE, M.R.F; et al . Solos com morfologia latossólica e caráter câmbico na região de Governador Valadares, Médio Rio Doce, Minas Gerais: gênese e micromorfologia. **Rev. Bras. Ciênc. Solo**, Viçosa , v. 32, n. 1, p. 259-270, Feb. 2008.

ARNFIELD, A. J. **Köppen climate classification**. Encyclopedia Britannica, 11 Nov. 2020, Disponível em : https://www.britannica.com/science/Koppen-climate-classification Accessed em 14 abril de 2021.

BARBOSA, et al. FUNÇÃO DA ÁGUA COMO TAMPÃO TÉRMICO PARA OS SERES VIVOS,. In: **Anais do Encontro Anual da Biofísica 2019**. São Paulo: Blucher, 2019. p. 183-184. ISSN 2526--607-1, https://doi.org/10.5151/biofisica 2019-57

BALDU, M. C. **Variabilidade pluviométrica e dinâmica atmosférica na bacia hidrográfica do rio Ivaí – PR. 2006**. 153 f. Tese (Doutorado em Geografia) – Universidade Estadual Paulista-UNESP, Presidente Prudente, SP, 2006.

BATALHA, M.A . O cerrado não é um bioma**. Biota Neotrop**., Campinas, v. 11, n. 1, p. 21-24, Mar. 2011.

BECKER, T.S et al. Efeito da Implantação e dinâmica do uso do solo sobre parâmetros biofísicos da Superfície no Assentamento Rural Roseli Nunes Em Mato Grosso. Raega- **O Espaço Geográfico em Análise**, v. 48, p. 153-166, 2020.

BEZERRA, et al. Análise da Temperatura de Superfície e do Índice de Vegetação no Município de Belém na Identificação das Ilhas de Calor. **Revista Brasileira de Cartografia**, v. 70, n. 3, p. 803-818, 2018.

BORGES, V; OLIVEIRA,D ; OLIVEIRA, R. Levantamento do diferencial térmico entre os municípios da bacia hidrográfica do rio paraibuna – mg/rj, pelo sensor termal do satélite landsat 5. **Periódico Eletrônico Fórum Ambiental da Alta Paulista**. p.6 (2010).

CARNEIRO, R.G. **Perfil da temperatura do solo nos biomas florestais da Amazônia e Mata Atlântica com aplicação da transformada em ondoletas**. 2014. 79f. Dissertação (Mestrado em Meteorologia) – Universidade Federal de Campina Grande, Campina Grande, 2014.

COELHO, A. L. N; CORREA, W, S. C. Temperatura de Superfície Celsius do Sensor TIRS/Landsat-8: metodologia e aplicações. **Revista Geográfica Acadêmica**, v. 7, n. 1, p. 31-45, 2013.

CRUZ, G.C.F. **A correlação entre vegetação e temperatura de superfície terrestre em ponta grossa-pr**. 8º Simpósio de Gestão Ambiental e Biodiversidade. PONTA GROSSA, PR. 2019

ENVI: **Processamento Digital.** Porto Alegre. Sulsoft. 2021. Disponível em:< http://www.envi.com.br/>

ESPINDOLA, H. S. Vale do Rio Doce: Fronteira, industrialização e colapso socioambiental. Fronteiras: Journal of Social, Technological and Environmental Science, v. 4, p. 160, 2015. https://doi.org/10.21664/2238- 8869. 2015v4i1. p160-206

FAVERO, C. **Uso e degradação de solos na microrregião de Governador Valadares, Minas Gerais. 2001**. 80 f. Tese (Doutorado em Solos e Nutrição de Plantas) - Universidade Federal de Viçosa, Viçosa. 2001.

FERREIRA, A.B; FILHO, W.P. Avaliação da reflectância espectral de corpos d'água em santa maria-rs por meio de espectrorradiometria de campo. **Geoambiente On-Line**. Jatai. Goias. 2009.

FERREIRA, T. R. et al. The use of remote sensing for reliable estimation of net radiation and its components: a case study for contrasting land covers in an agricultural hotspot of the Brazilian semiarid region. **Agricultural and Forest Meteorology**, v. 291, p. 108052-108070, 2020.

GUSSO, A; FONTANA,F.C; GLAUBER, A.G: Mapeamento da temperatura da superfície terrestre com uso do sensor AVHRR/NOAA." **Pesquisa agropecuária brasileira** 42.2 (2007): 231-237.

Hyams, D. G., CurveExpert software, http://www.curveexpert.net, 2020.

HUETE, A. R. A Soil-Adjusted Vegetation Index (SAVI). **Remote Sensing of Environment**, v. 25, n. 3, p.205-309, Aug. 1988

HUETE, A.R; LIU, H.Q. An error and sensivity analysis of the atmospheric and soil-correcting variants of the NDVI for the MODIS-EOS. IEEE **Transactions on Geoscience and Remote Sensing**, 32(4):897-905,1994.

Instituto Brasileiro de Geografia e Estatistica. Geociencias. *In*: **Geociencias**. [*S. l.*], 2020. Disponível em: https://www.ibge.gov.br/geociencias/downloads-geociencias.html Acesso em: 15 jun. 2021.

KÖPPEN, W. Climatologia con un estudio de los climas de la tierra. Mexico: Fundo de Cultura Economica, 1948. 478 p.

MARQUES, J. R.; FONTANA, D.; MELLO, R. W. Estudo da correlação entre a temperatura da superfície dos oceanos Atlântico e Pacífico e o NDVI, no Rio Grande do Sul. **Rev. bras. eng. agríc. ambient.**, Campina Grande, v. 9, n. 4, p. 520-526, Dec. 2005.

MICROSOFT EXCEL. Office. Comdex, Las Vegas. 2016.

MOREIRA, F.M.S; SIQUEIRA, J.O. **Microbiologia e Química do Solo**. 2. ed. Lavras: Lavras, 2006. 774 p.

OKE, T. R. Boundary layer climates. 2ed. New York: **Routledge**. 435 p.

PEREIRA, C.C. et al. Análise da temperatura de superfície e do uso da Terra e cobertura vegetal na bacia Barra dos Coqueiros (Goiás). **REVISTA GEONORTE**, Ed. 2, V.2, N.5, p.1243 – 1255, 2012.

PILLAR, V.D. 1995. **Clima e vegetação**. UFRGS, Departamento de Botânica.

PIRES, E. G; VALLERIUS, D.M. Distribuição Espaço-Temporal Da Temperatura De Superfície No Estado Do Rio Grande Do Sul. **Boletim Geográfico do Rio Grande do Sul**, n. 36, p. 105-129, 2020.

PMSB – Plano Municipal de Saneamento Básico. Produto 2 – Diagnóstico da Situação da Prestação dos Serviços de Saneamento Básico: Caracterização Geral do Município. Prefeitura Municipal de Governador Valadares, Governador Valadares, 2015. Disponível em: < https://www.valadares.mg.gov.br/abrir_arquivo.aspx/Diagnostico_caracterizacao_geral_do_municipio?cdLocal=2&arquivo=%7B64DC8181-E112-B640-6A1B-ACE07ED43A42%7D.pdf>. Acesso em 19 de novembro de 2021.

QGIS Development Team, 2009. **QGIS Geographic Information System**. Open Source Geospatial Foundation. URL http://qgis.org

SILVA, L.G; GALVINCIO, J.D. Análise Comparativa da Variação nos Índices NDVI e SAVI no Sítio PELD – 22, em Petrolina – PE, na Primeira Década do Século XXI. **Revista Brasileira de geografia física**. 2012

STEINKE,A,V; et al. Estimativa Da Temperatura De Superfície Em Áreas Urbanas Em Processo De Consolidação: Reflexões E Experimento Em Planaltina-Df**. Revista Brasileira de Climatologia**, [S.l.], v. 6, june 2010. ISSN 2237-8642.

SOARES, L. C. S; NASCIMENTO, A. R; QUEIROZ, B. S.C. **Correlação da temperatura de superfície e o índice de vegetação ajustado ao solo – SAVI.** XXIV Encontro Latino-Americano de Iniciação Científica, XX Encontro Latino Americano de Pós-Graduação e X Encontro de Iniciação à Docência - Universidade do Vale do Paraíba. 2020.

USGS – United States Geological Service. Using the USGS Landsat 8 Product. Disponível em: . Acesso em: 12. out. 2016.

WENG, Q.; FU, P.; GAO, F. Generating daily land surface temperature at Landsat resolution by fusing Landsat and MODIS data. **Remote Sensing of Environment**, v. 145, p. 55-67, 2014.

XU, J; TAN, W. (2007). The relationship between land surface temperature and NDVI with remote sensing: Application to Shanghai Landsat 7 ETM+ data. **International Journal of Remote** Sensing. 28.3205-3226.10.1080/01431160500306906.

ZEVIANI, Walmes Marques**. Parametrização Interpretativa em modelos não lineares**. 2013. 150 f. TESE (Doutorado em Estatística e experimentação agropecuária) - Universidade Federal de Lavras, Lavras, 2013